ASSOCIAZIONE NAZIONALE ITALIANA DI INGEGNERIA SISMICA ANIDIS
Italian National Association of Earthquake Engineering
XVIII CONVEGNO ANIDIS
L'ingegneria sismica in Italia
ASCOLI PICENO 2019
15-19 Settembre

Influence of traffic-induced vibrations on a rapid repairing material for bridge decks

Marinella Fossetti[a], Tullio Giuffrè[a], Giuseppe Macaluso[a], Alfio Francesco Siciliano[a], Giuseppe D'Arenzo[a], Rosario Davide Cottonaro[a]
[a] *Faculty of Engineering and Architecture, "Kore" University of Enna, Cittadella Universitaria - 94100 Enna (Italy)*

Keywords: Retrofitting of bridge decks, high performances mortars, vehicular traffic, influence of vibrations on the mechanical properties, experimental study.

ABSTRACT
Maintenance of bridge decks is an issue that Italy feels very strongly nowadays. High performances mortars are often used, especially during the extraordinary maintenance, in order to improve the structural performance of the decks but, the change of their mechanical properties caused by vehicular-induced vibrations has been little studied till now. For this reason, the circulation of vehicles is generally limited or interrupted during the maintenance activities, thereby increasing the costs of transport such as, for example, delays, higher emissions of pollutants into the atmosphere or increased risk of accidents etc.
In this context, the aim of the present study is to provide some experimental information, deducted by an "innovative" test procedure, about the influence of the vehicular traffic vibrations on the curing of high performance mortars.
To this end, the mechanical behaviour of specimens subjected to vibrations during the curing and that of specimens kept in static conditions are compared. The vibrations were applied by means a six degree of freedom hydraulic shaker and the input was made from acceleration data detected on some real bridges. Cubic, cylindrical and prismatic specimens have been used for the experimental tests. The critical analysis of the results show that the traffic induced vibrations change the mechanical characteristics of mortars analyzed.

1 INTRODUCTION

Rehabilitation of bridges on advanced life cycle represented one of the major challenges in field of road infrastructural networks (Malerba 2014). Maintenance activities or static and seismic retrofitting designs of the existing bridges are nowadays need in order to confront deterioration of the concrete, corrosion of the steel reinforcement and the significant increase of road traffic volume.

Economic and social activity development of any modern country depends on safety of road networks. In this regard, the maintenance of bridges and viaducts requires a major commitment both from the economic and the engineering point of view (Robak et al. 2015).

If the repairing process of existing bridges takes place without their complete closure it is possible to maintain efficient traffic flows and to reduce economic losses due to the increase of transport costs. In this case, the repair materials, as high-performance mortars, are subjected to vibrations induced by vehicle-traffic during the setting processes. Therefore, the influence of vibrations on the mechanical properties of these materials requires extensive studies.

The effects of the vehicle-induced vibrations on the early-age concrete have been studied over the years: Manning (1981); Harsh and Darwin (1986); Dunham et al. (2007); Fernandes et al. (2011); Wei et al. (2014) and Hong and Park (2015).

These studies evaluated, by experimental studies, the influence of vehicle-induced vibrations on the mechanical properties of concrete. However, the randomness of the vehicle traffic vibrations needs to be deepened. Many experimental tests were conducted considering simple harmonic forcing (Harsh and Darwin, 1986, Dunham et al. 2007; Fernandes et al. 2011) or certain vehicle traffic recording (Wei et al. 2014) due to technological limits of test set-up; they do not take into account the high variability of the signals in the time, frequency domain and their effects on the mechanical properties of the repair materials. Indeed, vibration recordings of vehicle-traffic present a wide frequency content which cannot be easily reproducible (Robak et al. 2015; Munasinghe et al. 1995). Moreover, experimental tests which use single vibration recordings do not consider the variability of geometric characteristics of different decks or the number of spans of bridges.

This paper aims to investigate the influence of vehicle-traffic vibrations on the mechanical properties of high-performance mortars for bridge repairs with an innovative test procedure; dynamic input is defined taking into account the randomness of recordings of vehicle-traffic vibrations, the variability of geometric dimension of decks and number of spans of bridges. Such signal is applied to specimens through a six degree-of-freedom shaker which allows to simulate vibrations with high frequency content.

Furthermore, the influence of the mortars age is also studied. Experimental tests were conducted on vibrated and not-vibrated (control) specimens, considering two mortars with different type of reinforced fibres. Finally, compressive and tensile flexural behaviour of control and vibrated specimens were evaluated for each type of mortar and comparisons in terms of mechanical properties are carried out.

2 PRELIMINARY ISSUES ABOUT MANAGEMENT FOR BRIDGES REPAIRING OPERATIONSS

Transportation agencies recently have an increasing interest in asset management because infrastructures support economic development of a nation, meets recreational and social needs, boosts public health and safety, and promotes sustainability (Robak et al. 2015). Moreover, the rate of economic growth and development tends to slow down when reconstruction is required (Munasinghe et al. 1995).

As bridges and viaducts are critical to the transportation infrastructure, their maintenance is essential in order to keep their desired serviceability and safety level, but these activities may also warrant the closure.

In fact, it is current practice that vehicles are rerouted to the shortest alternative route in terms of distance during bridge closures or when there is need for functional improvements. Furthermore, bridge preservation has a limited budget assigned because they have to compete for resources with other transportation infrastructure elements, such as pavements, rail lines, and ports.

Therefore, studies such as Zhang and Gao (2012) or Elbehairy et al. (2006) focused on determining better maintenance alternatives for bridge decks in order to extend the lifespan and decrease their expected life costs.

Nevertheless, they all attempted to maximize the benefit and minimize the cost and, although this approach may temporarily contain the effects of closures, they do not take into account the increasing user costs due to detours and the regional or the network impact caused.

In addition to this, detour routes may have limited lane capacity hence may only accommodate a portion of rerouted traffic volume.

In this context, the present study aims to provide a contribution on new economical assessments to carried out ordinary and/or extraordinary maintenance of bridges without suspended the circulation of vehicles. This problem is particularly important in these days because many bridges have now concluded their life cycle and the national bridge stock has showed several cases of collapsed bridges in the last decade (Calvi et al. 2018, Zordan, 2018).

3 EXPERIMENTAL PROGRAM

In order to verify the effects of vehicle-traffic vibrations on the curing of high-performance mortars, a comparison between some mechanical properties of 44 vibrated and not-vibrated (control) specimens is carried out.

One-component cementitious, thixotropic pre-mixed mortar is used. It is composed of sulphate-resistant hydraulic binders, organic corrosion inhibitors, expansive additives and it was mixed with water in a 100 l mixer. Furthermore, 0.25% of additive has been added to the mortars to reduce problems concerning the shrinkage.

Mortar was mixed with two type of fibres with the following mechanical properties:

- Structural polymer fibres (Mortar M1): Young modulus 4.5 GPa; Tensile strength 480 MPa; Length 25 mm; Diameter 540 μm.
- Polyacrylonitrile synthetic fibres and inorganic fibres (Mortar M2): Young modulus 72 GPa; Tensile strength 1700 MPa; Length 12 mm; Diameter 14 μm.

Experimental program is structured as follows:

- Hydrostatic weighing in according to EN 12390-7, 2002 to evaluate the mass density;
- Ultrasonic tests in according to EN 12504-4, 2005 to evaluate the modulus of elasticity;

– Compression tests according to EN 12390-3, 2003 on cubic specimens with size equal to 150 mm, to evaluate the compressive strength;
– Flexural tests according to EN 14651, 2007 on prismatic specimens with dimension equal to 150x150x600 mm, to estimate the tensile flexural behaviour.

The following nomenclature will be adopted: M1 or M2 defines the type of mortar while third letter identify the setting technique (C for control and V for vibrated specimens).

4 DYNAMIC INPUT

In this paper it is assumed that the deck vibrates with its own frequencies during the passage of vehicles because we considered vehicle actions like an ideal impulsive force that, as is well known, is characterized by a constant energy content at all frequencies from zero to infinity. For this reason, it is possible to draw relationships between the Power Spectral Density (PSD) function of the input $S_F(\omega)$ and the PSD of the output $S_X(\omega)$ by means of the square of the transfer function ($|H(\omega)|^2$)

$$S_X(\omega)=|H(\omega)|^2 S_F(\omega) \tag{1}$$

The decks considered in this study are constituted by reinforced concrete simply supported beams with different cross-section dimensions and different number of spans. Moreover, being that transfer function assumes different values along the beam, in order to define a generic dynamic input, three points are considered along the longitudinal axis of the decks: the midspan point and two points located respectively at L/3 and L/4 from one of the ends, L being the length of the deck. Therefore, results in terms of PSD of the acceleration evaluated in these three points and for different decks are combined in unique envelope PSD function. It allows to take into account the contribution of main first three modes of vibrations. Moreover, to take into account different kinds of decks, several PSD functions are evaluated.

It is a common knowledge that the area under the PSD curve is the variance of the acceleration; its square root, namely the standard deviation, is directly correlated to the maximum value of acceleration generated from the PSD by means of MonteCarlo simulation. Therefore, once the shape of the PSD has been defined starting from the dynamic characteristics of the considered decks, the ordinates are scaled in order to obtain a maximum acceleration amplitude equal to the maximum vertical acceleration that occurs in real cases.

The acceleration signals were obtained from relevant scientific literature (Castellaro et al. 2016a; Castellaro 2016b) and the maximum values ranging from 20-40 cm/s^2.

In order to cover some other possible uncertainty, the PSD was scaled to obtain a maximum peak equal to 200 cm/s^2.

5 VIBRATION DEVICE

Vibrations were applied to the specimens for eight hours (setting time) by means of a six degree-of-freedom shaker provided by the Team Corporation Ltd., model CUBE™ 2-DV-LS available in the Experimental Dynamics Laboratory in the L.E.D.A. facility (Fossetti et al. 2017). It is able to reproduce multi-axial vibration by means of six hydraulic actuators located inside the cube. The main applications of the CUBE™ shaker it is possible to perform a random test with assigned PSD in multi-axial configuration.

The test is controlled by a Control System which operates in the frequency domain and multi-channel (multi-axial). Several accelerometers were placed on the CUBE™ faces in order to monitor the test results. It is also worth noting that the system constituted by the mould full of mortar was undergone to a modal analysis to verify that the own frequencies of the system are far from those generated by the CUBE™ during the experimental test.

Figure 1 shows a view of the test set-up after the cast of the mortars.

Figure 1. Experimental set-up for evaluating the influence of vehicle-induced vibrations.

6 EXPERIMENTAL RESULTS

Control specimens were allocated in the same room of the Team CUBE™ shaker (see Figure 1) so that to reproduce the same environmental conditions with the vibrated specimens during the setting time. After the casting, all specimens were covered with a polyethilene sheet to avoid the rapid evaporation of the mixture water. Specimens were demoulded after 24 h and were cured in water at the temperature of 20°C.

6.1 Hydrostatic weighing

Mass density of control and vibrated specimens was determined for different days of curing. In particular, mass density D_{cm} was evaluated by the following expression

$$D_{cm} = \rho_w \frac{m_a}{m_a - \left[\left(m_{st} + m_w\right) + m_{st}\right]} \quad (2)$$

where ρ_w denotes the mass density of the water at 20°C, assumed equal to 998 kg/m^3, m_a is the specimen mass, m_{st} is the hook mass while m_{st}+ m_w is the system apparent mass recorded in the water.

The obtained results are in agreement with existing studies (Coppola et al. 2011, Unterweger et al. 2014) that showed that polymeric and inorganic fibres do not change the mass density and Young's modulus of mortar.

Furthermore, mass density is also subject to negligible change induced from vibrations. In fact, total average mass density of the M1 mortar is 2116.42 kg/m3 and 2117.44 kg/m3 for vibrated and control samples respectively while, it is 2171.38 kg/m3 and 2181.94 kg/m3 in the M2 mortar case.

6.2 Ultrasonic test

The method allows to estimate the dynamic modulus of elasticity through knowledge the time spent by the acoustic wave to cross the elastic medium as follow

$$E_d = \frac{(1\text{-}\nu)(1\text{-}2\nu)}{(1\text{-}\nu)} D_{cm} V^2 \quad (3)$$

where ν is the Poisson's ratio, assumed equal to 0.20 and V denotes the pulse propagation speed obtained from the pulse transit times directly measured on two opposing faces of specimen. Therefore, modulus of elasticity of the specimen was evaluated as

$$E_o = \frac{E_d}{1.062} \quad (4)$$

Finally, the E_{om} value was evaluated as average of E_o values measured by two different couples of faces of each specimen.

E_{om} was determined for different days of curing and the experimental results (see Table 1) show that control specimens of M1 mortar have modulus of elasticity greater than vibrated ones where, the average percentage variation of E_{om} between control specimens and vibrated decreases from 8.06% to 1.33% for 3 and 28 days of curing respectively. For M2 mortar, there are not significant differences between vibrated and control specimens.

Table 1. E_{om} of vibrated and control specimens in Mpa.

	Days of age	E_{om} control specimens	E_{om} vibrated specimens
M1	3	33187.75	29129.61
		30626.25	30324.07
		36426.11	32709.73
	10	39028.87	38616.35
		39238.13	37733.94
		39176.04	37653.96
	28	40706.91	38929.27
		39803.68	40106.91
		40187.65	40059.93
M2	3	37178.38	38162.54
		37895.73	37858.19
	10	39324.47	40646.34
		40226.46	39080.55
		38977.69	40256.34
	28	44059.38	42107.68
		42657.35	43133.24
		38471.39	40803.06

Table 2 synthetize the average modulus of elasticity E_{om} values of M1 and M2 mortars at 28 days of curing.

Table 2. Average values of E_{om} in MPa at 28 days of curing.

Type of mortar	E_{om} control specimens	E_{om} vibrated specimens
M1	40232.75	39698.70
M2	42014.66	41729.37

6.3 Uniaxial compression test

Compression tests were conducted at 3, 10, 28 ± 1 days of curing. Maximum machine load is 3000 kN. Experiments were carried out at a stress rate of 0.5 MPa/s. The compressive strength R_c was calculated as the ratio of axial load and the cross-section area of specimen.

The failure mode and crack patterns for each specimen was in accordance with UNI EN 12390-3 (2003). However, it worth to mention that structural polymer fibres in M1 mortar, improve the matrix performance during the post cracking stage, prevent spalling at failure and so a more controlled crack opening at each load stage was observed, as already highlighted in Afroughsabet et al. (2016). On the contrary, induced vibrations do not have influence on the failure mode for both mortars.

Compressive tests results are showed in Table 3. Three specimens were tested for each type of mortar, for the two setting conditions and for different curing days. Average compressive strength (R_{cm}) is assumed as the representative compressive strength from which, comparing the results obtained for M1 and M2 mortars, is possible conclude that peak stress values are not strongly influenced from the fibres type as shown in other studies (Coppola et al. 2011, Unterweger et al. 2014). Furthermore, it can be observed that induced vehicle-traffic vibrations reduce the compressive strength. This reduction concern both mortars and it increases with curing time. In particular, R_{cm} reduction at 28 days of age is equal to 11.69% and 11.43% for M1 and M2 mortar, respectively.

It is important highlighted that the results do not agree with previous studies in which the vibration characteristics did not derive by real bridges (Manning 1981, Fernandes et al. 2011), while they are in accordance with the studies conducted by Hong and Park (2015) in which vibrations input of an actual bridge were used.

6.4 Flexural test

Three points bend tests were performed to evaluate tensile flexural behaviour of the mortars. The tests were conducted to 28 ± 1 curing days and they consist on applying a centre-point load on a simply supported notched prism presented in Figure 2. Flexural strength of refer to some crack mouth opening displacements (CMOD) established in advance.

Tensile flexural strength $f_{ct,L}$ is calculated as

$$f_{ct,L} = \frac{3\,F_L\,l}{2\,b\,h_{sp}^2} \tag{5}$$

while residual tensile flexural strengths $f_{R,j}$ (with j = 1,2,3,4) are evaluated by the expression

$$f_{R,J} = \frac{3\,F_j\,l}{2\,b\,h_{sp}^2} \tag{6}$$

where F_L is the maximum value of load within the range CMOD 0÷0.05 mm while F_j is the load corresponding to $CMOD_j$ ($CMOD_1$=0.5 mm; $CMOD_2$=1.5 mm; $CMOD_3$=2.5 mm; $CMOD_4$= 3.5 mm); b is the width of the specimen; h_{sp} is the distance between the notch tip and the upper side; l is the span length of the specimen. Geometrical details are shown in Figure 2.

A machine with a maximum load of 150 kN was used for the three points bend tests. It is able to work in controlled manner i.e. producing a constant rate of displacement, and with sufficient stiffness to avoid unstable zones in the Load-CMOD curve.

A displacement transducer was installed on a rigid frame which is fixed to the test specimen at mid-height over the supports.

Tests are carried out applying displacements increments with 0.05 mm/s of speed. All specimens were loaded until the failure.

Moreover, since in an infrastructure it is important to have a repair material which is able to mitigate the adverse effects as the impact loads, two mechanical properties related to the post-cracking behaviour are evaluated: fracture energy G_F and fracture toughness K_{IC}.

Table 3. Compression tests results in MPa.

		3 days of age		10 days of age		28 days of age	
		R_c	R_{cm}	R_c	R_{cm}	R_c	R_{cm}
M1	(C)	45.94		54.69		75.30	
		43.56	43.33	56.31	56.25	73.59	74.34
		40.50		57.75		74.14	
	(V)	43.92		55.84		65.76	
		49.55	45.97	52.17	53.20	65.02	65.65
		44.45		51.59		66.18	
M2	(C)	57.28		57.45		71.02	
		54.59	55.94	61.15	58.28	79.84	73.78
		---		56.24		70.47	
	(V)	52.40		62.53		65.98	
		52.42	52.41	59.37	60.55	64.64	65.35
		---		59.74		65.42	

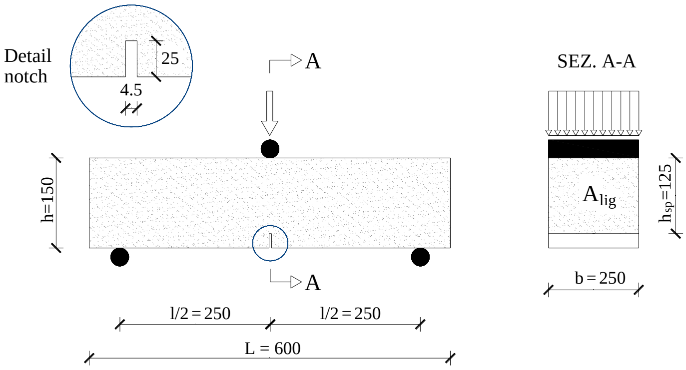

Figure 2. Details of experimental set-up of the three-points bending loading.

G_F was evaluated in according with RILEM 1985 TC50-FMC as follows

$$G_F = \frac{W_0 + m_b\, g\, \delta_0}{A_{lig}} \tag{7}$$

where W_0 is fracture work, m_b is the weight of the specimen between two supports; *g* is gravity acceleration, δ_0 is the span-deflection of specimen at failure and A_{lig} is ligament area shown in Figure 2. Although the method proposed in RILEM (1985) was originally used to evaluate the G_F for plain concrete, later it was used by several authors for fibres reinforced height performance mortar (Nguyen et al. 2018).

Fracture toughness K_{IC} was estimated in according to Engineering Fracture Mechanics 1990 as follows

$$K_{IC} = \sigma_n \sqrt{a_e}\, Y(\alpha) \tag{8}$$

where $\sigma_n = 6M/(b\,d^2)$, $M = \left[P_{max} + (\rho_l\, l/2) \right](l/4)$, P_{max} is the maximum load and ρ_l is self-weight of the specimen per unit length.

For calculation of the effective notch depth a_e in Eq (8) it was necessary to evaluate the Young's modulus E_m by Eq (9) estimated as in Nguyen et al. (2018). In Eq (9), in addition to the known symbols, P_i is arbitrary load level in the initial slop of the load-deflection curve; δ_i is its corresponding deflection; *a* is initial notch depth. The value of a_e was derived from Eq. (9) substituting P_i by P_{max} and δ_i by δ_p where, δ_p the mid-span deflection at peak load.

$$E_m = \frac{0.416\, P_i}{\delta_i} \left[\frac{l^3 \left(1 + \frac{5\, \rho_l\, l}{8\, P_i}\right)}{4\, b\, h^3 \left(1 - \frac{a}{h}\right)^3} + \frac{1.17\, l}{1.68\, b\, h \left(1 - \frac{a}{h}\right)} \right] \tag{9}$$

Finally, in Eq. (10), the correction factor $Y(\alpha)$ was calculated considering $\alpha = a_e/h$ by the following expression as in Nguyen et al. (2018)

$$Y(\alpha) = \frac{1.99 - \alpha(1-\alpha)(2.15 - 3.93\alpha + 2.70\alpha^2)}{(1+2\alpha)(1-\alpha)^{1.5}} \tag{10}$$

The failure mode and crack patterns obtained for vibrated and control specimens are in accordance with UNI EN 14651 (2007).

It was observed that the induced-vibrations have negligible effects on the failure mode.
M1 and M2 specimens failed in two different modes in accordance to that observed in the literature (Khitab et al. 2013, Unterweger et al. 2014).

(a)

(b)

Figure 3. Crack patterns after three points bend tests: Mortar M1 (a); Mortar M2 (b).

M1 failure mode was mainly governed by the collapse of the bonding between concrete paste and fibres (Figure 3a) and therefore it failed with a more controlled crack opening at each load stage, showing a more ductile failure than M2 specimens.

This beneficial effect is due of the structural polymer fibres. Series M2 failed with a large crack and a brittle failure (Figure 3b).

Load–CMOD curves for M1 and M2 specimens are shown in Figure 4 and Figure 5 respectively. The curves show quite clearly an initial linear-elastic branch up to the formation of first cracks, later following a nonlinear load-deflection pattern.

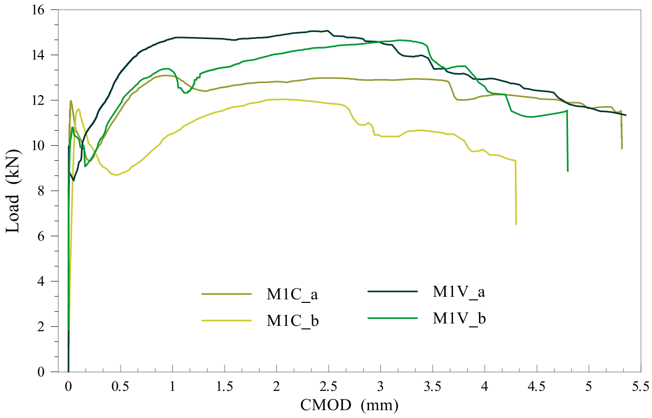

Figure 4 - Mortar M1: Load – CMOD curves.

It can be observed that all types of fibres added to the mortar have little-to-no effect on the ascending part of the Load-CMOD relationship but structural polymer fibres in M1 have also a significant effect on the post-peak branch, improving the ductility.

Comparing M1 and M2 Load-CMOD curves the change of failure mode from brittle mode into ductile mode can be observed by the post-peak behaviour.

In series M1, in which structural polymeric fibres crossing the crack, acting on the fibre–matrix bonding, the post-crack stress is larger than the cracking load, resulting in the strain hardening behaviour.

In series M2 the mortar exhibits strain softening behaviour, which represent the condition in which the damage localizes immediately after initiation of the first crack.

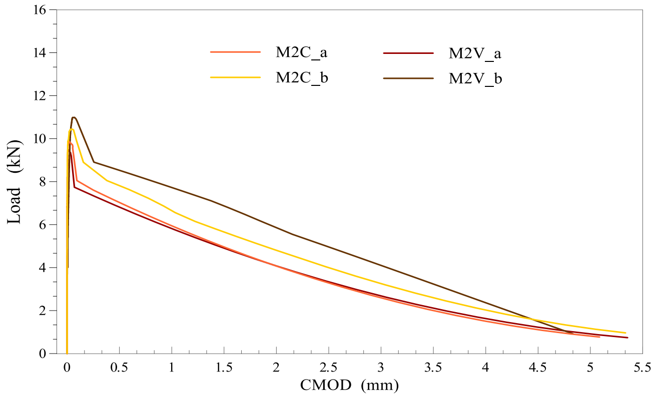

Figure 5 - Mortar M2: Load – CMOD curves.

Table 4 and Table 5 show the tensile flexural results and residual tensile flexural strength deduced from experimental data by using Eq. (5) and Eq. (6).

Table 4 - Tensile flexural strength in MPa

		Tensile flexural strength	
		$f_{ct,L}$	$f_{ct,Lm}$
M1	(C)	3.83	3.47
		3.11	
	(V)	3.19	3.32
		3.46	
M2	(C)	3.15	3.25
		3.34	
	(V)	3.03	3.27
		3.50	

For example, total average value of the residual strengths ($f_{R,jm}$) increase of about 20% than of the tensile strength ($f_{ct,Lm}$) in M1 mortar, while quickly decrease in series M2.

Regarding the influence of vibrations, for both mortars, it is evident that they do not induce significant variations on $f_{ct,Lm}$, while increase $f_{R,jm}$.

Table 5. Residual tensile flexural strength in MPa.

		$f_{R,1}$	$f_{R,2}$	$f_{R,3}$	$f_{R,4}$	$f_{R,1m}$	$f_{R,2m}$	$f_{R,3m}$	$f_{R,4m}$
M1	(C)	3.70	4.03	4.15	4.13	3.25	3.87	3.97	3.76
		2.80	3.71	3.79	3.40				
	(V)	4.23	4.70	4.82	4.36	4.01	4.50	4.70	4.38
		3.79	4.30	4.59	4.41				
M2	(C)	2.23	1.62	1.06	0.61	2.37	1.71	1.14	0.73
		2.51	1.80	1.22	0.84				
	(V)	2.15	1.56	1.02	0.68	2.44	1.89	1.27	0.86
		2.73	2.23	1.53	1.04				

In mortar M1, the increase of the residual tensile flexural strength of vibrated specimens respect to control one is of 23.43%, 16.49%, 18.38% and 16.45% respectively for $f_{R,1}$, $f_{R,2}$, $f_{R,3}$ and $f_{R,4}$.

In mortar M2, this increase is of 2.86%, 10.46%, 11.72% and 18.28% respectively for $f_{R,1}$, $f_{R,2}$, $f_{R,3}$ and $f_{R,4}$.

Therefore, in general, it is possible to assert that the induced vibrations do not negatively influence the tensile flexural behaviour of high-performance mortars M1 and M2 for concrete repairing.

This result is confirmed also for the values of fracture energy G_F and fracture toughness K_{IC} showed in Table 6. In fact, for mortar M1, the vibrated specimens increase average fracture energy and fracture toughness roughly about 15% than control specimens. Furthermore, it can be observed that the type of fibres in the mortar play a fundamental role on the G_F and K_{IC} values.

Table 6. Fracture energy and Fracture toughness.

		fracture energy G_F N/mm	fracture toughness K_{IC} MPa mm$^{1/2}$
M1	(C)	2.58	48.48
		2.27	43.78
	(V)	2.25	54.01
		3.35	50.96
M2	(C)	0.90	20.84
		1.20	22.88
	(V)	0.91	18.95
		1.07	26.34

In conclusion, it is possible to assert that, the structural polymer fibres in M1 appear to increase the values of fracture energy G_F and fracture toughness K_{IC} when subjected to vehicle-induced vibrations. Probably, induced vibration on the fresh mortar favours the alignment of the structural fibres making them perpendicular to the notch, hence in tensile stress direction. However, more experimentally studies are necessary to generalized the results.

7 CONCLUSIONS

In this paper the effects of vehicle-traffic vibrations on high performance mortars for bridge repairs were studied through an innovative test device, a six degree-of-freedom shaker, which allows to assign a power spectral density function in multi-axial configuration. Furthermore, the dynamic input was defined taking into account the randomness of vehicle-traffic vibrations recorded in actual bridges, the variability of geometric dimensions of decks and number of spans of actual bridges.

Experimental tests, based on 44 cubic and prismatic specimens, were conducted comparing the compressive and tensile flexural behaviour of control and vibrated specimens.

Fibres indicated for the repair of bridge are used in the mortars: structural polymer fibres in mortar M1 and polyacrylonitrile synthetic fibres and inorganic fibres in mortar M2.

Fibres effects showed in the experimental results are in accordance with the literature. Indeed, mass density, modulus of elasticity and compressive strength have a negligible change. The principal fibres induced effects can be observed on the flexural behaviour of the specimens. In fact, structural polymer fibres in M1 mortar resulted in a more controlled propagation of cracks, tending to reduce the sudden failure of specimen, and in a significative increase in the flexural strength, fracture and toughness energy of mortar. The reason is that, after matrix cracking, the structural fibres carry the load until the interfacial bond between fibres and matrix is broken.

Vehicle-induced vibrations effects obtained in the experimental campaign are shown below:

– They do not significantly change mass density and modulus of elasticity;
– Compression behaviour in the early curing days is not significantly altered but it decreases around 12% after 28 days. These results do not agree with the findings of previous studies in which the vibration characteristics did not derive by real bridges. While, these results are in accordance with the experimental results of Hong and Park (2015) that used a dynamic input obtained from an actual bridge.
– They appear do not have detrimental effect on tensile flexural properties. In particular, it was observed that induced vibrations increase residual tensile flexural behaviour, probably because they produce the fibres alignment on the fresh mortar. However, more experimentally studies are necessary to drawing more general conclusions.
– Structural polymer fibres embedded in M1 mortar improve the ductility and hence the seismic behaviour of both mortar and the repaired decks.

Although further investigations should be accomplished to generalize results obtained from the present experimental study, they provide a contribution on the bridges repair designs assessments.

In particular, the following recommendation should be followed: if the repair design concerns that the compressive strength is improved by means of a high performance mortars, it is necessary to take in to account the detrimental effect induced by the traffic vibrations; if the vehicle vibrations occur within the first hours of the life of a repaired bridge decks, they can have a significant effect on its remaining life.

Based on these results, the early age behaviour of bridge decks repaired with a high-performance mortars and subjected to vehicle-traffic vibrations must be further investigated in order to answer to new economical assessments about ordinary and/or extraordinary maintenance of bridges without suspended vehicles circulation.

ACKNOWLEDGEMENTS

Authors would express their gratefulness to the personnel of Experimental Dynamics Laboratory in the L.E.D.A. facility of Enna, for their activities. In particular, Prof. Giacomo Navarra and Prof. Francesco Lo Iacono are gratefully acknowledged.

REFERENCES

Afroughsabet V., Biolzi L., Ozbakkaloglu T., 2016. High-performance fiber-reinforced concrete: a review, *Journal of Materials Science*, **51** (14), 6517-6551.

Calvi G.M., Moratti, M., O'Reilly G.J., Scattarreggia, N., Monteiro, R., Malomo, D., Calvi, P.M., Pinho, R., 2018. Once upon a Time in Italy: The Tale of the Morandi Bridge, *Structural Engineering International*, DOI: 10.1080/10168664.2018.1558033, 20 pp.

Castellaro S., 2016a. Soil and structure damping from single station measurements, *Soil Dynamics and Earthquake Engineering*, 90, 480-493.

Castellaro S., Barrasso P., Isani S., 2016b. Validazione del modello MIDAS di un viadotto per mezzo di caratterizzazione dinamica speditiva effettuata con Tromino, *Structural Modeling CSPFEA*, 13/14, 26-33.

Coppola L., Cadoni E., Forni D., Buoso A., 2011. Mechanical Characterization of Cement Composites Reinforced with Fiberglass, Carbon Nanotubes or Glass Reinforced Plastic (GRP) at High Strain Rates. *Applied Mechanics and Materials*, 82, 190-195.

Dunham M.R., Rush A.S., Hanson J.H., 2007. Effects of Induced Vibrations on Early Age Concrete. *Journal of Performance of Constructed Facilities*, 179-184.

Elbehairy H., Elbeltagi E., Hegazy T., Soudki K., 2006. Comparison of Two Evolutionary Algorithms for Optimization of Bridge Deck Repairs. *Computer-Aided Civil and Infrastructure Engineering*, **21**(8), 561-572.

EN 12390-7:2002, 2002. Testing hardened concrete, Density of hardened concrete.

EN 12390-3, 2003. Testing hardened concrete. Compressive strength of test specimens.

EN 12504-4, 2005. Testing concrete Part 4: Determination of ultrasonic pulse velocity.

EN 14651, 2007. Test method for metallic fibre concrete – Measuring the flexural tensile strength (limit of proportionally (LOP), residual).

Fernandes J.F., Bittencourt T.N., Helene P., 2011. Concrete subjected to vibrations in early-ages. *Ibracon Structures and Materials Journal*, 592-609.

Fossetti M., Lo Iacono F., Minafò G., Navarra G., Tesoriere G., 2017. A new large-scale laboratory: the LEDA Research Centre (Laboratory of Earthquake engineering and Dynamic Analysis). Proc. of Intern. Conf. 7aese, Pavia, 6-8 Sept. Publisher: *EUCENTRE Foundation*.

Harsh S., Darwin D., 1986. Traffic-Induced Vibrations and Bridge Deck Repairs. *Concrete International*, 36-42.

Hong S., Park S., 2015. Effect of vehicle-induced vibrations on early-age concrete during bridge widening. *Construction and Building Materials*, 77, 179–186.

Khitab A., Arshad M.T., Hussain N., Tariq K., Ali S.A., Kazmi S.M.S., Munir M.J., 2013. Concrete reinforced with 0.1 vol% of different synthetic fibers. *Life Science Journal*, 10 (12s), 934-939.

Malerba P.G., 2014. Inspecting and repairing old bridges: experiences and Lessons. *Structure and Infrastructure Engineering: Maintenance, Management, Life-Cycle Design and Performance*, **10**(4), 443–470.

Manning D.G., 1981. Effects of traffic-induced vibrations on bridge-deck repairs. NCHRP Synthesis; No. 86, *Transportation Research Board*, Washing·ton, D.C., 40 pp.

Munasinghe M., Clarke C.L., World B., 1995. International Decade for Natural Disaster, R. Disaster prevention for sustainable development: economic and policy issues. *International Decade for Natural Disaster Reduction and World Bank*, Washington, DC.

Nguyen H., Carvelli V., Adesanya E., Kinnunen P., Illikainen M., 2018. High performance cementitious composite from alkali-activated ladle slag reinforced with polypropylene fibers. *Cement and Concrete Composites*, 90, 150–160.

RILEM 1985 TC 50-FMC, 1985. Determination of the fracture energy of mortar and concrete by means of three-point bend tests on notched beams, *International Union of Laboratories and Experts in Construction Materials, Systems and Structures*, 287-290.

Robak A., Monkman D., Gilberston T., Bush S., O'Connor, B., Blakemore, R., Garlik, S., Hughes, J., Gordon, M., Sharman B., Smith M., Maughan A., Onley D., Belgrove T., Waugh R., Holland G., Roberts L., Way P., Dever-Tod K., Lutchman R., and Holdt C.V., 2015. IIMM International Infrastructure Management Manual 2015. *Institute of Public Works Engineering Australasia* (IPWEA), New Zealand.

Unterweger C., Brüggemann O., Fürst C., 2014. Short-Fiber-Reinforced Polypropylene Composites: Comparison of Different Reinforcing Fibers. *Chemiefasertagung Dornbirn* (Dornbirn-MFC), Dornbirn, Austria.

Wei W., Shuo L., Qizhi W., Wei Y., Mingzhang C., Xiaotian H., Shuai M., Xuanyu L., 2014. The Impact of Traffic-Induced Bridge Vibration on Rapid Repairing High-Performance Concrete for Bridge Deck Pavement Repairs. *Advances in Materials Science and Engineering*, 9 pp.

Zhang X., Gao H., 2012. Determining an Optimal Maintenance Period for Infrastructure Systems. *Computer-Aided Civil and Infrastructure Engineering*, **27**(7), 543-554.

Zordan T., 2018. From the Morandi Bridge to the Namawukulu Footbridge: A Clear Message of Commitment from IABSE. *Structural Engineering International*, **28**(4), 393-393.